
Comparative Biodistribution of Iodinated Amino Acids in Rats: Selection of the Optimal Analog for Oncologic Imaging Outside the Brain

Tony Lahoutte, MD; John Mertens, PhD; Vicky Caveliers, PharmD, PhD; Philippe R. Franken, MD, PhD; Hendrik Everaert, MD, PhD; and Axel Bossuyt, MD, PhD

Department of Nuclear Medicine, Academic Hospital, Free University Brussels, Jette, Belgium

3-¹²³I-Iodo- α -methyltyrosine (¹²³I-3-IMT) is used for the detection of residual and recurrent brain tumors. The application of ¹²³I-3-IMT for the study of extracerebral malignancies is limited by its marked and rapid renal uptake. In this study, we compared the tumor uptake, biodistribution, and specificity of 5 structurally related iodinated amino acids with those of ¹²³I-3-IMT. The aim was to select the optimal analog for oncologic imaging outside the brain. **Methods:** We studied 3-¹²³I-iodotyrosine (¹²³I-3-IT), 2-¹²³I-iodotyrosine (¹²³I-2-IT), ¹²³I-iodo-azatyrosine (¹²³I-IAzaT), 2-¹²³I-iodophenylalanine (¹²³I-2-IPhe), and 4-¹²³I-iodophenylalanine (¹²³I-4-IPhe). Tumor uptake and renal uptake in sarcoma-bearing rats were measured by use of *in vivo* dynamic imaging. The differential uptake ratio (average counts per pixel of the region of interest divided by the average counts per pixel inside the total body) and rates of tracer accumulation (K_1 values) were calculated. Results were compared with the values obtained for ¹²³I-3-IMT in the same rat. Tracers that demonstrated high tumor uptake were labeled with ¹²⁵I and coinjected with ¹⁸F-FDG in rats with turpentine-induced acute inflammation. After 30 min, the rats were sacrificed and dissected. Amino acid tracer uptake in organs and tissues was measured, and the increase in uptake in the inflamed muscle was expressed relative to the increase in ¹⁸F-FDG uptake. **Results:** Tumor uptake and K_1 values for ¹²³I-2-IT and ¹²³I-2-IPhe were comparable to those for ¹²³I-3-IMT. ¹²³I-4-IPhe showed high tumor uptake but a reduced K_1 value because of high blood-pool activity. ¹²³I-3-IT and ¹²³I-IAzaT did not accumulate markedly in tumor tissue. Renal accumulation of ¹²³I-2-IT, ¹²³I-2-IPhe, and ¹²³I-4-IPhe was at least 6 times lower than that of ¹²³I-3-IMT. ¹⁸F-FDG uptake was markedly increased in areas of acute inflammation (215%). The increases for ¹²⁵I-3-IMT and ¹²⁵I-4-IPhe were 35.5% and 22.2%, respectively, of the increase for ¹⁸F-FDG. Almost no increase was found for ¹²⁵I-2-IT (3.3%) and ¹²⁵I-2-IPhe (2.8%). **Conclusion:** ¹²³I-2-IT and ¹²³I-2-IPhe are promising tracers for oncologic imaging outside the brain. ¹²³I-2-IT has the advantage of an established kit for radiosynthesis.

Key Words: amino acids; tumor imaging; inflammation; biodistribution; small-animal imaging

J Nucl Med 2003; 44:1489–1494

Received Jan. 16, 2003; revision accepted Apr. 21, 2003.
For correspondence or reprints contact: Tony Lahoutte, MD, Department of Nuclear Medicine, Academic Hospital, Free University Brussels (AZ-VUB), Laarbeeklaan 101, 1090 Jette, Belgium.
E-mail: tony.lahoutte@az.vub.ac.be

Amino acid tracers are mainly used for the study of brain tumors. High tumor uptake and low physiologic uptake in gray matter result in clear images that surpass those obtained with ¹⁸F-FDG (1,2). The accumulation reflects the increased amino acid transport (AAT) activity of cancer cells (3). A few reports have demonstrated that certain amino acid tracers are accumulated less by inflammatory cells, suggesting that increased AAT accumulation is more tumor specific than increased glucose accumulation (4–6). Such specificity is of utmost importance for the study of residual and recurrent tumor tissues after primary therapy. Therefore, it would be interesting to study AAT status by use of PET or SPECT of suggestive lesions in the follow-up after therapy (7). However, amino acid imaging of extracerebral tumors has not been explored extensively (8,9).

3-¹²³I-Iodo- α -methyltyrosine (¹²³I-3-IMT) is the main tracer used to study AAT by SPECT. Its application in the abdominal area is limited by its marked and rapid renal accumulation. The aim of this study was to compare 5 structurally related iodinated amino acids and to select the analog with the best characteristics for the study of residual or recurrent malignant disease outside the brain. The parameters used were tumor uptake, biodistribution, and uptake into inflammatory tissue. Tumor uptake and biodistribution for the analogs were compared with those for ¹²³I-3-IMT. Uptake of the analogs in areas of inflammation was compared with that of ¹⁸F-FDG.

MATERIALS AND METHODS

Laboratory Animals

For the tumor model, male Wag/Rij rats ($n = 5$) were subcutaneously injected in the right flank with 10^6 R1M rhabdomyosarcoma cells (Harlan Nederland). Tumors were grown for 4 wk. For the inflammation model, male Wag/Rij rats ($n = 12$) were injected in the left calf muscle with 0.15 mL of turpentine. Two rats with a tumor were also injected with turpentine for a combined tumor–inflammation model. Inflammation experiments were performed 24 h after turpentine injection. The animals had free access to water and food until 4 h before tracer injection. The animals were anesthetized with halothane. Afterward, the animals were sacrificed by intravenous injection of KCl. The study protocol was

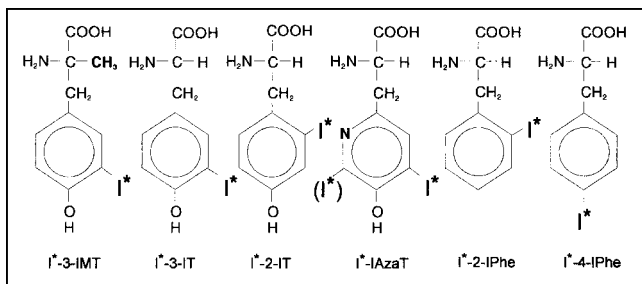


FIGURE 1. Chemical structures of iodinated amino acid analogs under investigation.

approved by the ethical committee for animal studies of our institution, and National Institutes of Health principles of laboratory animal care (NIH publication 86-23, revised 1985) were followed.

Radiopharmaceuticals

¹²³I- or ¹²⁵I-3-IMT. Radioiodination of L- α -methyltyrosine (Sigma-Aldrich) with ¹²³I or ¹²⁵I (Nordion Europe) was performed by carrier-added electrophilic substitution with IODO-GEN (Pierce Europe) as an oxidizing agent. The reaction was performed at 0°C, and the reaction mixture was mixed for 2 min, yielding >90% ¹²³I- or ¹²⁵I-3-IMT. ¹²³I- or ¹²⁵I-3-IMT was separated from the starting molecule by use of a small reverse-phase C₁₈ Sep-Pak column (Waters) as described by Gühlke and Biersack (10). A radiochemical purity of >99% was obtained.

^{3,123}I-Iodotyrosine (¹²³I-3-IT) and ¹²³I-Iodo-Azatyrosine (¹²³I-IAzaT). Radioiodination and purification of L-3-iodotyrosine and L-iodo-azatyrosine (Sigma-Aldrich) were performed as described for ¹²³I-3-IMT, yielding >95% ¹²³I-3-IT and >98% ¹²³I-IAzaT. A radiochemical purity of >99% was obtained.

^{2,123}I- or ¹²⁵I-Iodotyrosine (¹²³I- or ¹²⁵I-2-IT). Radioiodination of 0.5 mg of L-2-iodotyrosine (ABX) was performed by Cu⁺-assisted nucleophilic exchange under acidic and reducing conditions (0.5 mg of SnSO₄, 5 mg of gentisic acid, 12 mg of citric acid, and 0.325 mg of CuSO₄·H₂O) at 120°C for 60 min, yielding >98% ¹²³I- or ¹²⁵I-2-IT and a radiochemical purity of >98%.

^{4,123}I- or ¹²⁵I-Iodophenylalanine (¹²³I- or ¹²⁵I-4-IPhe). Radioiodination of L-4-iodophenylalanine (Sigma-Aldrich) was performed by Cu⁺-assisted nucleophilic exchange as described above, yielding 98% ¹²³I- or ¹²⁵I-4-IPhe and a radiochemical purity of >98%.

^{2,123}I- or ¹²⁵I-Iodophenylalanine (¹²³I- or ¹²⁵I-2-IPhe). Radioiodination of 0.5 mg of L-2-bromine-phenylalanine was performed by Cu⁺-assisted nucleophilic exchange as described above, yielding >98% ¹²³I- or ¹²⁵I-2-IPhe. Purification by semipreparative reverse-phase high-pressure liquid chromatography (C₁₈ column [250 × 10 mm]; 5% acetonitrile–95% H₂O–0.1% trifluoroacetic acid; 6 mL/min) followed by preconcentration and recovery from a C₁₈ Sep-Pak column cartridge resulted in a final radiochemical purity of >98%.

The chemical structures of the iodinated amino acids are shown in Figure 1.

¹⁸F-FDG. ¹⁸F-FDG was produced by nucleophilic fluorination.

Dynamic Planar Imaging

Tumor, renal, and blood-pool activities as functions of time for the various ¹²³I-labeled amino acid analogs were measured by dynamic imaging with a gamma camera equipped with a medium-energy collimator (the resolution was 11.1 mm at full width at half maximum). Imaging was started immediately after intravenous injection of 18.5 MBq of the appropriate tracer. A total of 240 images of 10 s each were acquired in 128 × 128 matrices with a zoom factor of 3.2 (pixel size, 1.5 mm) and a photopeak window set at 15% around 159 keV. In order to reduce variability between different animals, we investigated each rat with ¹²³I-3-IMT (reference) and 1 or 2 of the other tracers on different days. Images were corrected for remaining ¹²³I activity from the previous day by use of a static acquisition of 5 min before tracer injection.

Regions of interest (ROIs) were manually drawn around the tumor, the contralateral background area, the left ventricle of the heart, the right kidney, and the total body. The injected dose was defined as the total number of counts inside the total body. Tracer uptake was calculated as the differential uptake ratio (DUR; average counts per pixel in the ROI divided by average counts per pixel inside the total body) and plotted as a function of time. For comparison of the various tracers, the area under the curve (AUC) was calculated for the DUR curves between 10 and 40 min after injection. The ratio of the AUC for the tested amino acid tracer to the AUC for ¹²³I-3-IMT obtained in the same rat was calculated for comparison. Similarly, ratios of tumor uptake to background uptake were plotted as a function of time and, for comparison, AUC ratios were calculated.

Patlak Analysis

A Patlak analysis of the data from the first 7 min, carried out by use of the counts inside the heart as the input function, was

TABLE 1
Comparison of Tested Amino Acid Tracers with ¹²³I-3-IMT (Reference)

Tracer	Tumor		Kidney		Heart DUR	T/BKG
	DUR	K ₁	DUR	K ₁		
¹²³ I-2-IT	1.03	1.09	0.25	0.10	1.12	0.95
¹²³ I-AzaT	0.70	0.45	0.24	0.08	1.48	0.47
¹²³ I-3-IT	0.65	0.50	0.42	0.31	1.30	0.60
¹²³ I-2-IPhe	0.97	0.94	0.16	0.07	0.92	0.85
¹²³ I-4-IPhe	1.06	0.63	0.38	0.13	1.51	0.65

DUR values represent ratio of AUC for tested amino acid tracer to AUC for ¹²³I-3-IMT in same rat. K₁ values represent ratio of K₁ value for amino acid tracer to K₁ value for ¹²³I-3-IMT in same rat. T/BKG values represent ratio of AUC for tumor uptake (T) to AUC for background uptake (BKG).

performed for the calculation of rates of tracer uptake (K_1 values) for tumor accumulation and renal accumulation by use of the following equation:

$$\frac{T(t)}{H(t)} = K_1 \frac{\int_0^t H(t) \cdot dt}{H(t)}$$

The graph of this equation yields a straight line with a slope equal to the K_1 value (11,12). For renal accumulation, $T(t)$ is substituted by $R(t)$. The ratio of the K_1 value for the tested amino acid tracer to that for ^{123}I -3-IMT obtained in the same rat was calculated for comparison.

Biodistribution and Accumulation into Areas of Inflammation

Tracers that demonstrated high tumor accumulation in the imaging study were selected for the biodistribution study carried out by use of Wag/Rij rats with turpentine-induced inflammation. The animals were injected with 5 MBq of one of the ^{125}I -labeled amino acid tracers together with 37 MBq of ^{18}F -FDG and then sacrificed at 30 min after injection. The organs and tissues were removed rapidly, washed, and weighed. Muscle tissues were collected from the inflamed left leg and noninflamed right leg. The radioactivity of the samples was counted by use of a γ -counting system (Cobra Inspector 5003; Canberra Packard). ^{18}F activity was counted on day 1, and ^{125}I activity in the same samples was counted 3 d later. The amount of radioactivity in the tissue was expressed as the differential absorption ratio (activity per gram of sample divided by the activity injected per gram).

The increase in accumulation in the inflamed muscle versus the noninflamed muscle was calculated. The increase in ^{18}F -FDG accumulation for individual rats was regarded as a measure of the degree of induced inflammation. The increase in the accumulation of the amino acid tracers was expressed as a percentage of the increase in the uptake of ^{18}F -FDG in the same rat.

Dynamic PET Imaging

Two rats with coexisting tumor and turpentine-induced inflammation were studied. The first rat underwent a dynamic planar imaging study after ^{123}I -3-IMT injection and then a dynamic ^{18}F -FDG PET study. The second rat underwent a dynamic planar imaging study after ^{123}I -2-IT injection and then a dynamic ^{18}F -FDG PET study. Dynamic planar imaging was performed as described above. PET imaging was performed immediately after intravenous injection of 10 MBq of ^{18}F -FDG with an LSO-PET camera (ACCEL-Siemens; the resolution was 6.4 mm at full width at half maximum). A total of 40 images of 60 s each (40 min) were acquired. Images were reconstructed iteratively (32 subsets, 10 iterations), and all coronal slices were reprojected in 2 dimensions for image quantification. ROIs were drawn over the inflamed muscle, the contralateral noninflamed muscle, the tumor, and the total body. The DUR as a function of time was calculated for the different ROIs. The DUR in inflamed muscle versus that in noninflamed muscle was plotted as a function of time for the amino acid and ^{18}F -FDG studies.

Statistical Analysis

We studied the behavior of different tracers in the same rat, always including a reference tracer (^{123}I -3-IMT or ^{18}F -FDG) to reduce variability between different animals (tumor size and

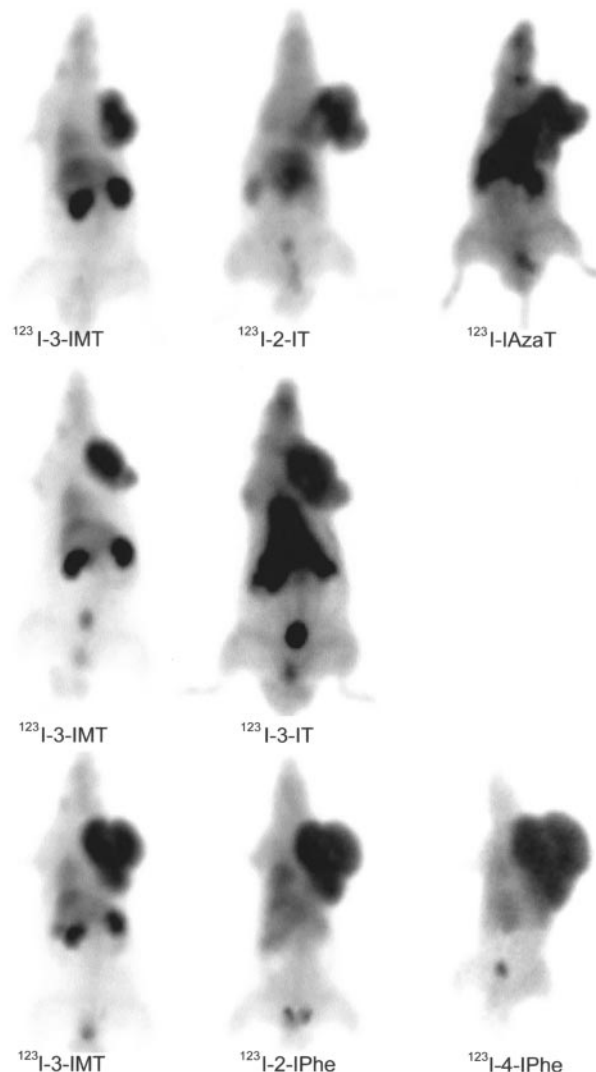


FIGURE 2. Summed images (30–40 min after injection) from dynamic planar imaging study. Images are scaled to maximum in tumor.

amount of inflammation). The results are expressed as the average and the SD or range as appropriate.

RESULTS

Dynamic Planar Imaging

Tumor uptake of ^{123}I -2-IT, ^{123}I -2-IPhe, and ^{123}I -4-IPhe was comparable to that of ^{123}I -3-IMT (Table 1). ^{123}I -3-IT and ^{123}I -IAzaT tumor uptake was low. Renal activity was high for ^{123}I -3-IMT but considerably lower for the other amino acid tracers. Blood-pool activity was highest for ^{123}I -4-IPhe and ^{123}I -IAzaT. The rate of tracer entering the tumor (K_1 value) for ^{123}I -2-IT and ^{123}I -2-IPhe was comparable to that for ^{123}I -3-IMT but was 37% lower for ^{123}I -4-IPhe. The correlation coefficients (R^2) of the Patlak analysis ranged from 0.91 to 0.98. The ratio of tumor uptake to background uptake for ^{123}I -2-IT was closest to that for

^{123}I -3-IMT. From this experiment, we selected ^{123}I -2-IT, ^{123}I -2-IPhe, and ^{123}I -4-IPhe for further study; ^{123}I -3-IT and ^{123}I -IAzaT were rejected because of their low tumor accumulation. The summed image (between 30 and 40 min after injection) for the 6 different tracers is shown in Figure 2.

Biodistribution and Accumulation into Areas of Inflammation

Comparative biodistribution data for ^{125}I -3-IMT, ^{125}I -2-IT, ^{125}I -2-IPhe, ^{125}I -4-IPhe, and ^{18}F -FDG are shown in Table 2. Marked pancreatic accumulation was measured for all amino acid tracers. Brain activity was high for ^{18}F -FDG but low for the amino acid tracers. Renal activity was very marked for ^{125}I -3-IMT but was at least 6 times lower for ^{125}I -2-IT, ^{125}I -2-IPhe, and ^{125}I -4-IPhe. Liver activity was comparable for the 4 amino acid tracers. Blood-pool activity was highest for ^{125}I -4-IPhe.

The increase in tracer accumulation in inflamed muscle versus noninflamed muscle was highest for ^{18}F -FDG (average, 215%). Relative to the increase in ^{18}F -FDG accumulation, the increases in amino acid accumulation in inflamed muscle were 35.5% (range, 15.6%–57.7%) for ^{125}I -3-IMT, 3.3% (range, 0.3%–6.2%) for ^{125}I -2-IT, 2.8% (range, 2.9%–7.6%) for ^{125}I -2-IPhe, and 22.2% (range, 16.9%–26.8%) for ^{125}I -4-IPhe.

Dynamic PET Imaging

The images of the ^{123}I -2-IT and ^{18}F -FDG PET studies of an R1M tumor-bearing rat with coexisting inflammation are shown in Figure 3. The ratios of tracer uptake in inflamed tissue to that in noninflamed tissue as a function of time for ^{18}F -FDG/ ^{123}I -3-IMT and ^{18}F -FDG/ ^{123}I -2-IT are shown in Figure 4. The ratio was initially higher for ^{123}I -3-IMT than for ^{18}F -FDG and stayed nearly constant as a function of time. The ratio was significantly lower for ^{123}I -2-IT than for

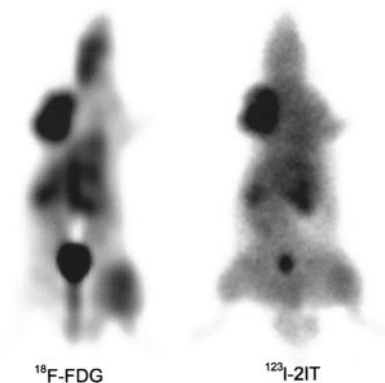


FIGURE 3. ^{18}F -FDG and ^{123}I -2-IT images from R1M tumor-bearing rat with coexisting inflammation (summed images at 30–40 min after injection).

^{18}F -FDG and decreased as a function of time. The tumor accumulation of ^{18}F -FDG was higher than that for the amino acid tracers; the DUR values were 1.43 for ^{18}F -FDG/ ^{123}I -3-IMT and 1.08 for ^{18}F -FDG/ ^{123}I -2-IT.

DISCUSSION

We compared the biodistribution data for 6 radioiodinated amino acid analogs by using in vivo dynamic imaging. In order to avoid variability between animals, different tracers were studied in the same rat and always with a reference tracer (^{123}I -3-IMT or ^{18}F -FDG). Tracers with high tumor accumulation were further investigated by dissection studies. The data showed that apparently small molecular modifications of the amino acid tracers resulted in important differences in biodistribution. The position of the iodine atom appears to be critical; a tyrosine molecule with an

TABLE 2
Biodistribution of 4 Amino Acid Analogs and ^{18}F -FDG in Wag/Rij Rats

Tissue	Mean \pm SD differential absorption ratio for:				
	^{125}I -3-IMT	^{125}I -2-IT	^{125}I -2-IPhe	^{125}I -4-IPhe	^{18}F -FDG
Blood	1.08 \pm 0.41	1.36 \pm 0.13	1.36 \pm 0.39	2.38 \pm 0.22	0.68 \pm 0.17
Heart	1.05 \pm 0.29	1.32 \pm 0.06	1.28 \pm 0.13	1.56 \pm 0.13	5.54 \pm 2.48
Lung	1.13 \pm 0.46	1.30 \pm 0.19	1.40 \pm 0.22	1.38 \pm 0.94	1.17 \pm 0.27
Liver	1.73 \pm 0.45	1.63 \pm 0.06	1.37 \pm 0.26	1.68 \pm 0.21	0.70 \pm 0.06
Spleen	0.87 \pm 0.18	1.44 \pm 0.01	1.39 \pm 0.40	1.73 \pm 0.19	1.67 \pm 0.23
Pancreas	3.35 \pm 0.69	5.31 \pm 0.55	3.80 \pm 0.17	5.84 \pm 0.09	0.43 \pm 0.06
Stomach	1.84 \pm 0.14	1.37 \pm 0.16	1.20 \pm 0.03	1.32 \pm 0.48	0.83 \pm 0.16
Small intestine	0.85 \pm 0.19	1.40 \pm 0.07	1.14 \pm 0.14	1.24 \pm 0.08	1.26 \pm 0.20
Large intestine	1.02 \pm 0.64	1.34 \pm 0.25	0.88 \pm 0.13	0.95 \pm 0.02	1.44 \pm 0.42
Bone	0.29 \pm 0.13	0.51 \pm 0.24	0.42 \pm 0.04	0.43 \pm 0.37	0.93 \pm 0.36
Brain	0.80 \pm 0.08	1.11 \pm 0.09	0.84 \pm 0.08	1.04 \pm 0.08	3.30 \pm 0.16
Kidney (right)	16.22 \pm 3.58	3.35 \pm 0.16	1.99 \pm 0.29	1.64 \pm 0.10	1.53 \pm 0.15
Kidney (left)	18.31 \pm 1.66	3.51 \pm 0.24	2.03 \pm 0.16	1.61 \pm 0.16	1.51 \pm 0.15
Muscle (noninflamed)	0.40 \pm 0.08	1.16 \pm 0.23	0.98 \pm 0.03	1.09 \pm 0.04	0.29 \pm 0.24
Muscle (inflamed)	0.71 \pm 0.14	1.25 \pm 0.04	1.11 \pm 0.16	1.50 \pm 0.08	0.83 \pm 0.16

$n = 3$ for amino acid tracers and $n = 12$ for ^{18}F -FDG.

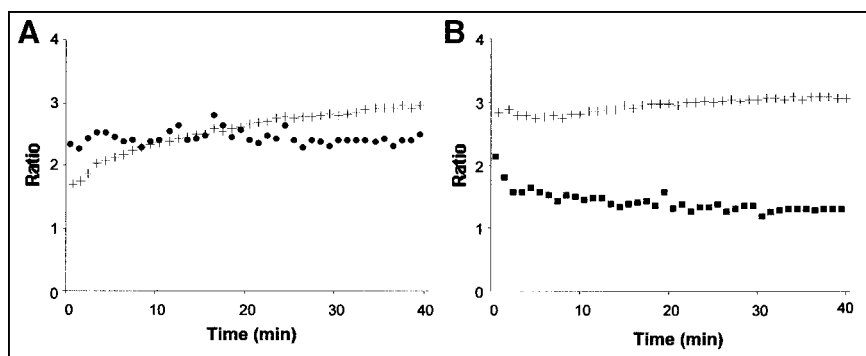


FIGURE 4. Ratio of tracer uptake in inflamed tissue to that in noninflamed tissue as function of time for ^{18}F -FDG (+) and ^{123}I -3-IMT (●) (A) and for ^{18}F -FDG (+) and ^{123}I -2-IT (■) (B).

iodine atom placed in the *ortho* position (^{123}I -2-IT) is markedly accumulated by a tumor, whereas tumor uptake is low when iodine is situated in the *meta* position (^{123}I -3-IT). However, when a methyl group is added to the α -carbon atom of ^{123}I -3-IT to yield ^{123}I -3-IMT, the molecule is once again accumulated in a tumor. The undesirable marked renal accumulation of ^{123}I -3-IMT is also linked to the α -carbon methyl group, as ^{123}I -3-IT is only weakly captured by the kidneys.

The uptake of ^{123}I -2-IT, ^{123}I -2-IPhe, and ^{123}I -4-IPhe was high in tumor tissue and low in the kidneys. However, the blood-pool activity of these tracers was higher than that of ^{123}I -3-IMT, especially for ^{123}I -4-IPhe. High blood-pool activity for ^{123}I -4-IPhe has been reported before (13,14) and reduced the ratio of tumor uptake to background uptake in our study. Again, the structural analog with the iodine in the *ortho* position (^{123}I -2-IPhe) has a more favorable biodistribution. The data suggest that the relatively large iodine atom induces the least amount of steric hindrance in the *ortho* position, preserving high-affinity recognition by AAT system L (see below). Because the affinity (K_m) of the amino acid tracers for the specific transporters is in the micromolar range and because endogenous levels of competing substrates are also in the micromolar range, we can exclude the possibility that nanomolar differences in tracer carrier concentrations attributable to different labeling methods had a significant influence on the quantitative measurements in our study.

As with the differences in biodistribution, we also found important differences in specificity. The acute inflammation induced by turpentine consists of a large number of granulocytes (15). ^{125}I -2-IT and ^{125}I -2-IPhe did not accumulate markedly in areas of acute inflammation, whereas ^{125}I -3-IMT and ^{125}I -4-IPhe showed significant accumulation. For ^{125}I -4-IPhe, this accumulation could have been caused by its high blood-pool activity. The reason for the significant ^{125}I -3-IMT accumulation in areas of inflammation is less clear. Nonspecific uptake of ^{125}I -3-IMT has been reported before (8,16,17). A possible explanation could involve the transporter subtype selectivity of the different analogs; AAT system L represents not a single transporter protein but a small family of transporter proteins (LAT1, LAT2, and others) with small differences in substrate recognition (18).

The differential expression of system L transporter subtypes on tumor cells and inflammatory cells was recently described (19). We speculate that different structural analogs prefer different transporter subtypes and that this characteristic may explain the important differences in biodistribution and specificity between ^{123}I -3-IMT and ^{123}I -2-IT or ^{123}I -2-IPhe. Therefore, it may not be correct to state that all radiolabeled amino acids are tumor specific; this characteristic depends on the type of transporter protein that is studied with the selected tracer.

Tumor accumulation of ^{18}F -FDG measured by PET was higher than tumor accumulation of ^{123}I -3-IMT and ^{123}I -2-IT measured by use of a gamma camera. This finding can be attributed partially to the lower resolution of the gamma camera, leading to an underestimation of tracer accumulation.

Some deiodination, demonstrated by thyroid uptake, was found on the images of ^{123}I -IAzaT. Metabolite or protein incorporation was not studied here. Previous experiments showed that ^{123}I -3-IMT and ^{123}I -2-IT are not metabolized and do not enter protein synthesis (20). The absence of metabolism of these iodinated analogs also has been attributed to the iodine atom, because analogs labeled with the much smaller fluorine atom do enter intracellular metabolic pathways and are incorporated into proteins (21).

CONCLUSION

^{123}I -2-IT and ^{123}I -2-IPhe are both promising tracers for oncologic imaging outside the brain because of their high tumor accumulation, low renal uptake, and minor accumulation into areas of acute inflammation. Because of low physiologic brain uptake, these tracers are also interesting for the detection of brain tumors. The ^{123}I -2-IT analog could be the best tracer for clinical studies because its chemical synthesis is relatively easy and can be performed with a kit formulation.

ACKNOWLEDGMENT

This work was supported by a grant from the Belgian Fonds voor Wetenschappelijk Onderzoek-Vlaanderen (FWO-VI).

REFERENCES

1. Weber W, Bartenstein P, Gross MW, et al. Fluorine-18-FDG PET and iodine-123-IMT SPECT in the evaluation of brain tumors. *J Nucl Med.* 1997;38:802–808.
2. Langen KJ, Ziemons K, Kiwit JC, et al. 3-¹²³I]Iodo-alpha-methyltyrosine and [methyl-¹⁴C]-L-methionine uptake in cerebral gliomas: a comparative study using SPECT and PET. *J Nucl Med.* 1997;38:517–522.
3. Jager PL, Vaalburg W, Pruim J, de Vries EG, Langen KJ, Piers DA. Radiolabeled amino acids: basic aspects and clinical applications in oncology. *J Nucl Med.* 2001;42:432–445.
4. Rau FC, Weber WA, Wester HJ, et al. O-(2-[(18)F]Fluoroethyl)-L-tyrosine (FET): a tracer for differentiation of tumor from inflammation in murine lymph nodes. *Eur J Nucl Med.* 2002;29:1039–1046.
5. Kubota K, Yamada S, Kubota R, Ishiwata K, Tamahashi N, Ido T. Intramural distribution of fluorine-18-fluorodeoxyglucose in vivo: high accumulation in macrophages and granulation tissues studied by microautoradiography. *J Nucl Med.* 1992;33:1972–1980.
6. Kubota R, Kubota K, Yamada S, et al. Methionine uptake by tumor tissue: a microautoradiographic comparison with FDG. *J Nucl Med.* 1995;36:484–492.
7. Weber WA, Dick S, Reidl G, et al. Correlation between postoperative 3-[(123)I]iodo-L-alpha-methyltyrosine uptake and survival in patients with gliomas. *J Nucl Med.* 2001;42:1144–1150.
8. Jager PL, Franssen EJ, Kool W, et al. Feasibility of tumor imaging using L-3-[iodine-123]-iodo-alpha-methyl-tyrosine in extracranial tumors. *J Nucl Med.* 1998;39:1736–1743.
9. Flamen P, Bernheim N, Deron P, et al. Iodine-123- α -methyl-L-tyrosine single photon emission tomography for the visualization of head and neck squamous cell carcinomas. *Eur J Nucl Med.* 1998;25:177–181.
10. Gühlke S, Biersack HJ. Simple preparation of L-3-iodo- α -methyl tyrosine suitable for use in kit preparations. *Appl Radiat Isot.* 1995;46:177–179.
11. Patlak CS, Goldstein DA, Hoffman JF. The flow of solute and solvent across a two-membrane system. *J Theor Biol.* 1963;5:426–427.
12. Peters AM. Graphical analysis of dynamic data: the Patlak-Rutland plot. *Nucl Med Commun.* 1994;15:669–672.
13. Samnick S, Hellwig D, Bader JB, et al. Initial evaluation of the feasibility of single photon emission tomography with p-¹²³I]iodo-L-phenylalanine for routine brain tumor imaging. *Nucl Med Commun.* 2002;23:121–130.
14. Samnick S, Richter S, Romeike BF, et al. Investigation of iodine-123-labelled amino acid derivatives for imaging cerebral gliomas: uptake in human glioma cells and evaluation in stereotactically implanted C6 glioma rats. *Eur J Nucl Med.* 2000;27:1543–1551.
15. Blankenberg FG, Tait JF, Blankenberg TA, Post AM, Strauss HW. Imaging macrophages and the apoptosis of granulocytes in a rodent model of subacute and chronic abscesses with radiolabeled monocyte chemotactic peptide-1 and annexin V. *Eur J Nucl Med.* 2001;28:1384–1393.
16. Kuwert T, Morgenroth C, Woesler B, et al. Uptake of iodine-123-alpha-methyl tyrosine by gliomas and non-neoplastic brain lesions. *Eur J Nucl Med.* 1996;23:1345–1353.
17. Dierickx LO, Lahoutte T, Deron P, et al. Diagnosis of recurrent head and neck squamous cell carcinoma with 3-¹²³I]iodo-L-alpha-methyltyrosine SPET. *Eur J Nucl Med.* 2001;28:282–287.
18. Verrey F, Jack DL, Paulsen IT, Saier MH Jr, Pfeiffer R. New glycoprotein-associated amino acid transporters. *J Membr Biol.* 1999;40:205–212.
19. Rau FC, Philippi H, Rubio-Aliaga I, et al. Identification of subtypes of amino acid transporters in human tumor and inflammatory cells by RT-PCR [abstract]. *J Nucl Med.* 2002;43(suppl):24P.
20. Lahoutte T, Caveliers V, Dierickx L, et al. In vitro characterization of the influx of 3-¹²³I]iodo-L- α -methyltyrosine and 2-¹²⁵I]iodo-L-tyrosine into U266 human myeloma cells: evidence for system T transport. *Nucl Med Biol.* 2001;28:129–134.
21. Wienhard K, Herholz K, Coenen HH, et al. Increased amino acid transport into brain tumors measured by PET of L-(2-[F-18])fluorotyrosine. *J Nucl Med.* 1991;32:1338–1346.

